

Annular aperture array based color filter

Guangyuan Si,¹ Yanhui Zhao,² Hong Liu,³ Siewlang Teo,³ Mingsheng Zhang,⁴
Tony Jun Huang,² Aaron J. Danner,^{1,a)} and Jinghua Teng^{3,b)}

¹Centre for Optoelectronics, Department of Electrical and Computer Engineering,
National University of Singapore, 4 Engineering Drive 3, Singapore 117576

²Department of Engineering Science and Mechanics, The Pennsylvania State University, University Park,
Pennsylvania 16802, USA

³Institute of Materials Research and Engineering, 3 Research Link, Singapore 117602

⁴Data Storage Institute, Spintronics, Media and Interface Division, 5 Engineering Drive 1, Singapore 117608

(Received 20 April 2011; accepted 10 June 2011; published online 20 July 2011)

In this letter, we propose and experimentally demonstrate a color filter based on an annular aperture geometry working in the visible range. The device is built by configuring an array of annular apertures in a gold film suitable for transmission measurement. We show effective fine tuning of resonance peaks through precise geometric control of the aperture dimensions. Selective transmission through annular apertures of various sizes leads to continuous color tuning of transmitted electromagnetic waves. This may find potential for application in high-definition displays, optical filters, ultrafast switching, and bio-sensing. © 2011 American Institute of Physics. [doi:10.1063/1.3608147]

Annular aperture arrays (AAAs) have generated extensive interest in the last decade because of their potential as an important candidate for ultracompact optical devices, after the extraordinary optical transmission (EOT) properties of such geometries were first reported by Baida and co-workers.¹ Early investigations of guiding light of wavelengths much larger than the waveguide aperture dimensions using AAAs have shown several interesting phenomena and peculiar optical properties.^{2–12} For example, the cutoff wavelength of a guided mode can be effectively shifted to longer wavelengths when the outer and inner radii are approaching each other.⁶ Additionally, the low group velocity of the fundamental mode leads to important applications when materials with high electro-optic coefficients (lithium niobate, for instance) are employed in the AAA design.¹³ Moreover, such coaxial structures can find application in composing single layer metamaterials in the visible range.^{14–16}

Very high (up to 90%) transmission through AAAs has previously been achieved at visible frequencies (using AAAs fabricated in a silver film¹⁷) and this property, combined with the fact that the optical response of AAAs is also insensitive to the incident angle,^{18,19} makes the AAA structure a perfect candidate for high efficiency display and filtering devices. Here, we propose a simple yet effective method to filter individual colors using AAA-based geometries. Fabrication of apertures with features as small as 25 nm that show efficient color-filter functionality is demonstrated. An effective wavelength selecting function with AAAs that can be operated across the whole visible band and tuning of transmission resonance via structural control are also demonstrated. The optical response of the fabricated devices can be precisely tailored by shaping the aperture gap width, leading to opportunities for nanophotonics and optics.

A two dimensional AAA structure usually has at least two transmission peaks, as reported by different groups under

different designs.^{1–6,10–12} The transmission peaks are caused by cylindrical surface plasmons (CSPs) and planar surface plasmons (PSPs),^{8,10–12} respectively. CSPs are affected by the geometrical design and the thickness of the metal film, while PSPs are mainly related to the periods of two dimensional gratings fabricated therein. The resonance peaks are a direct result of Fabry-Pérot resonances in a cylindrical resonance cavity formed by a metal film with finite thickness and two end-faces. For a finite metal film with thickness l , the design of the desired transmission peaks can be estimated by the following equation²⁰

$$l = \frac{m\pi - \varphi}{\beta} \quad (1)$$

where l is the thickness of the metal film, m is the order of the Fabry-Pérot resonance, and φ and β represent phase of reflection and propagation constant, respectively. For the case where l is constant, the propagation constant β varies with different annular aperture sizes and affects the reflection and transmission of the designed structure. Detailed discussion and analytical solutions of φ and β can be found elsewhere.²⁰

In our case, the target is to design a color filter which allows the transmission of a selected wavelength in the visible range for applications of true color or high-definition displays. Therefore, a metal film with fixed thickness is preferred. The periods of the two dimensional gratings also play an important role affecting the selective transmission. The enhanced transmission caused by two dimensional structures can be estimated as¹

$$\lambda = \frac{p_x p_y}{\sqrt{i^2 p_y^2 + j^2 p_x^2}} \sqrt{\frac{\varepsilon_m \varepsilon_d}{\varepsilon_m + \varepsilon_d}} \quad (2)$$

where p_x and p_y are periods of annular apertures along the x and y directions, respectively, ε_m and ε_d represent the permittivities of metal and dielectric, and i and j are integers. The

^{a)}Electronic mail: adanner@nus.edu.sg.

^{b)}Electronic mail: jh-teng@imre.a-star.edu.sg.

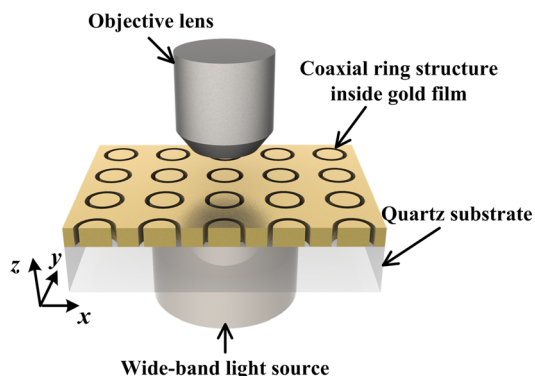


FIG. 1. (Color online) Schematic drawing of the proposed color filter working under transmission measurement.

position of the transmission peaks caused by PSPs is determined by the periods of the two dimensional gratings. Thus, it can be artificially tuned by changing the periods of the gratings. In our case, multiple transmission peaks within the visible range will degrade the performance of the color selector. We try to minimize this effect by increasing the periods of the two-dimensional gratings so that the resonance peaks can be moved out of the visible range. With fixed metal thickness and grating periods, our color selector is achieved by tuning the gaps of the AAAs only.

Figure 1 shows a schematic representation of the fabricated elements and measurement system in this work. Using electron-beam evaporation, a 160 nm thick Au film over a 6 nm Ti adhesion layer was first deposited on a quartz substrate. Then, arrays of coaxial rings were milled using focused ion beam (FIB) etching. Each array comprises 9×9 rings occupying an area of $\sim 10 \times 10 \mu\text{m}^2$. The inner radii of the coaxial rings are fixed to 200 nm while the outer radii change from 225 nm to 270 nm in steps of 15 nm (corresponding to a 25–70 nm gap width). Measurements of the transmission properties of the fabricated nanostructures were carried out using a UV-Vis-NIR microspectrometer (CRAIC QDI 2010) at normal incidence. A 75 W broadband xenon lamp was used as an unpolarized white light source. Transmission measurements were normalized with respect to a bare quartz substrate. Figures 2(a) and 2(b) show scanning electron microscope (SEM) images of a fabricated AAA, and a single aperture (gap width equal to 25 nm) with a much higher magnification, respectively. Figure 2(c) plots the measured transmission spectra of the coaxial structures with gap widths of 25, 40, 55, and 70 nm. One can see that when the gap width is 70 nm, a broad resonance can be observed which is centered at ~ 590 nm. After the gap is narrowed to 55 nm, the transmission peak shifts to around 650 nm in the spectrum. Further reducing the gap width to 40 and 25 nm, additional red shifts can be observed and resonance peaks are located at ~ 680 nm and 710 nm in the spectrum, respectively. Note that the tuning of transmission peaks was realized via controlling the gap width of the ring apertures instead of the periodicity (fixed to 1200 nm) of the arrays. The transmission characteristics are mainly determined by the CSP modes inside each gap cavity rather than by the periodicity.

To further investigate the underlying physical principles related to the annular apertures, we carried out FDTD simu-

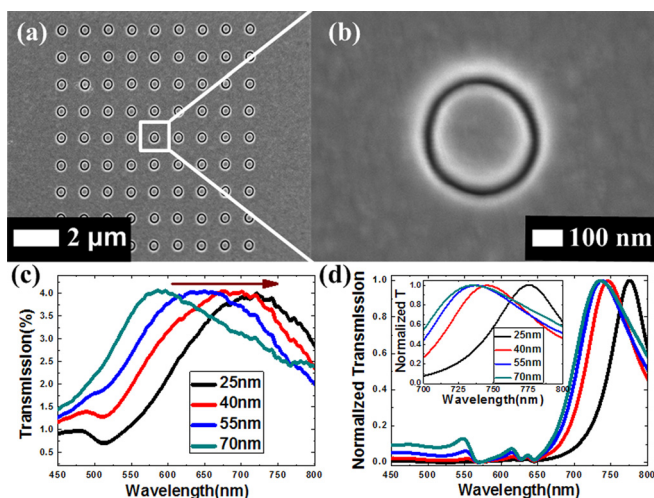


FIG. 2. (Color online) SEM images showing (a) overview of a fabricated 9×9 AAA and (b) magnified view of a single ring with 25 nm gap width. (c) Measured and (d) simulated transmission spectra of AAAs as a function of gap width. Simulated spectra are normalized for clarity. The apertures have fixed inner radius at 200 nm and varying outer radii from 225 nm to 270 nm in steps of 15 nm. The arrow in (c) indicates decreasing gap width. Inset of (d), magnified peak tops with 700–800 nm wavelength range to show the shift more clearly.

lations to investigate the theoretical performance of the structures. The dispersion model of gold was based on the Johnson and Christy model²¹ in the material library of the software. The dimension of the simulation area was $2.4 \mu\text{m} \times 2.4 \mu\text{m} \times 1 \mu\text{m}$, which allowed two periods of the ring structure in x-y plane and enough space for the light source and power monitors. We applied periodic boundary conditions for the x and y directions and perfectly matched layer (PML) boundary conditions for the z direction. Polarized Gaussian beams were used as the light source with the polarization direction along the x axis. A power monitor was located 300 nm above the Au film to collect any transmission modes reaching the output region. The calculated transmission spectra are shown in Fig. 2(d). The position of the resonance peaks strongly depends on the diameter values, and similar results have been observed and discussed in Refs. 6 and 11. Redshift of the resonance peaks can also be observed when decreasing the gap width. Note that the simulated transmission curves here are normalized to clearly show the shift trend of the transmission peaks. Compared to the measured spectra, the slightly smaller spectral width and red shift of the peak wavelength λ_{max} observed in the simulations are due to the difference between the idealized features used in the simulations and imperfect structures of fabricated elements for testing, e.g., rough surfaces and tapered sidewalls caused by redeposition during FIB milling.

The calculated electric field distributions are presented in Fig. 3. Strong confinement of light in the nanoring cavity is obvious, corresponding to the TE_{11} mode demonstrated in previous work.^{4,6} Top and cross-sectional views of the ring with 55 nm gap width at transmission maximum ($\lambda = 740$ nm) and transmission minimum ($\lambda = 600$ nm) confirm that the selective transmission is caused by the resonant ring cavities with various gap sizes.

In order to further tune the transmission response and finally filter individual colors out, AAAs with 40 nm

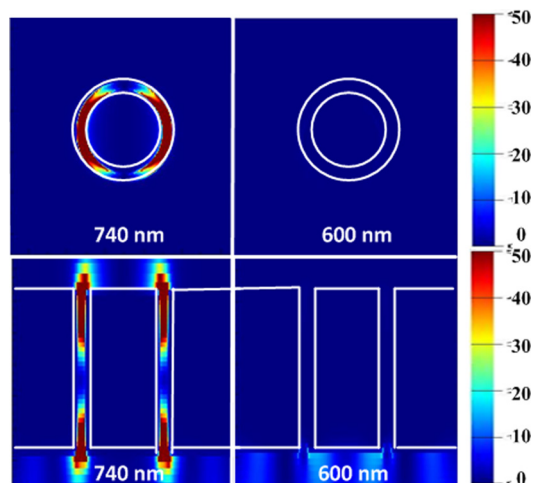


FIG. 3. (Color online) Top panel: top view and bottom panel: cross-sectional view showing the electric intensity distribution of a single ring with 55 nm gap width illuminated at 740 nm (λ_{\max}) and 600 nm (λ_{\min}).

increments were milled in another sample with significantly increased gap widths. SEM images of the fabricated structures are shown in Figs. 4(a)–4(d). Using 40-, 80-, 120-, and 160-nm-wide ring apertures, colors of red, yellow, blue, and cyan, respectively, are clearly observed in Fig. 4(e). As plotted in Fig. 4(f), resonances occur at different wavelengths when varying the gap widths; peaks gradually shift to longer wavelengths as the rings are narrowed. The relatively weak intensity is mainly caused by high loss and attenuation over a long propagation distance (160 nm Au with 6 nm Ti in this work). For arrays with 160 nm and 120 nm gaps, the transmission peaks are located at about 480 nm and 500 nm, giving cyan and blue colors, respectively. When the gap aperture is narrowed down to 80 nm, the peak shifts to ~ 600 nm, exhibiting a yellow color. More light at around 680 nm is transmitted when the gap is further narrowed to only 40 nm, which results in a red color. A similar trend has been observed in Fig. 2: a blue shift of the transmission peaks occurs with increasing sizes of the annular aperture.

In summary, we have demonstrated tuning of the transmission resonance at visible frequencies using AAAs in a gold film. The optical response of a broadband light source through coaxial rings is wavelength-selective and accurate control can be achieved to filter individual colors out. FDTD calculations confirm the resonance dependence of selective transmission on gap width. Using AAAs, fine tuning of optical response through structural control and a color filtering function under transmission mode can be readily realized, opening up opportunities for sensing and integrated optics.

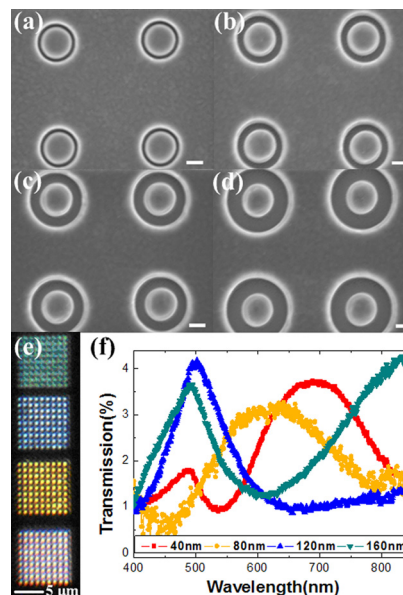


FIG. 4. (Color online) SEM images of the fabricated AAAs with (a) 40 nm, (b) 80 nm, (c) 120 nm, and (d) 160 nm gap width (outer radii equal to 240 nm, 280 nm, 320 nm, and 360 nm with 200 nm fixed inner radius). Scale bars are 200 nm. (e) Corresponding optical image presenting different colors. (f) Measured transmission spectra of the AAAs with different color outputs shown in (e).

The first two authors contributed equally to the work. This work was financially supported by Agency for Science, Technology and Research (A*STAR), under Grants No. 092 1540099 and 092 1540098.

- ¹F. I. Baida and D. Van Labeke, *Opt. Commun.* **209**, 17 (2002).
- ²F. I. Baida *et al.*, *Opt. Commun.* **256**, 190 (2005).
- ³F. I. Baida *et al.*, *Opt. Commun.* **282**, 1463 (2009).
- ⁴J. Salvi *et al.*, *Opt. Lett.* **30**, 1611 (2005).
- ⁵F. I. Baida and D. Van Labeke, *Phys. Rev. B* **67**, 155314 (2003).
- ⁶F. I. Baida *et al.*, *Phys. Rev. B* **74**, 205419 (2006).
- ⁷B. Heshmat *et al.*, *Opt. Express* **19**, 5912 (2011).
- ⁸S. M. Orbons *et al.*, *Opt. Lett.* **33**, 821 (2008).
- ⁹P. Banzer *et al.*, *Opt. Express* **18**, 10896 (2010).
- ¹⁰S. M. Orbons *et al.*, *Appl. Phys. Lett.* **90**, 251107 (2007).
- ¹¹M. I. Haftel *et al.*, *Appl. Phys. Lett.* **88**, 193104 (2006).
- ¹²M. I. Haftel *et al.*, *Phys. Rev. B* **74**, 235405 (2006).
- ¹³E. H. Barakat *et al.*, *Opt. Express* **18**, 6530 (2010).
- ¹⁴S. P. Burgos *et al.*, *Nat. Mater.* **9**, 407 (2010).
- ¹⁵R. de Waele *et al.*, *Opt. Express* **18**, 12770 (2010).
- ¹⁶F. J. Rodríguez-Fortuño *et al.*, *Opt. Lett.* **34**, 3325 (2009).
- ¹⁷Y. Poujet *et al.*, *Opt. Lett.* **32**, 2942 (2007).
- ¹⁸A. Belkhir and F. I. Baida, *Phys. Rev. E* **77**, 056701 (2008).
- ¹⁹D. Van Labeke *et al.*, *Opt. Express* **14**, 11945 (2006).
- ²⁰B. Heshmat *et al.*, *Opt. Express* **19**, 5912 (2011).
- ²¹P. B. Johnson and R. W. Christy, *Phys. Rev. B* **6**, 4370 (1972).